EXPERIMENTAL BEHAVIOUR OF LOW-RISE STEEL BUILDINGS WITH FLEXIBLE ROOF DIAPHRAGMS

Robert TREMBLAY[1], Tarek BERAIR[2] And André FILIATRAULT[3]

SUMMARY

This paper reports on an shake table test program performed at École Polytechnique of Montreal in which a low-rise steel building model with a flexible roof diaphragm was subjected to seismic ground motions. Several parameters were investigated among which the stiffness of the roof diaphragm, the ground motion characteristics, and in-plane mass, stiffness, and strength eccentricities. The paper presents the design of the model, including the similitude relationships developed for this particular application. The test results show that a simplified formula can be used to estimate the fundamental period of the structures. Under strong ground motion, in-plane roof deformations are approximately twice as large as those predicted with a static analysis. Shear forces measured in the diaphragm were also higher than those obtained assuming static loading conditions. Eccentricity is found to affect significantly the inelastic response of these structures.

INTRODUCTION

Figure 1 illustrates the main structural components of typical steel low-rise buildings. The weight of these structures is concentrated at the roof level and, therefore, horizontal inertia forces mainly develop at that level under seismic ground motions. These structures typically include a metal roof deck diaphragm and vertical steel bracing to resist these lateral loads. The roof diaphragm is made of steel deck units that are attached to each other and fastened to the supporting steel roof framing to form a deep horizontal girder capable of transferring the lateral loads to the vertical bracing elements. The vertical bracing transfers the loads from the roof level to the foundations. It is most often made of vertical trusses that are built by adding slender diagonal bracing members such as tie rods or flat bars within the beam-column system.
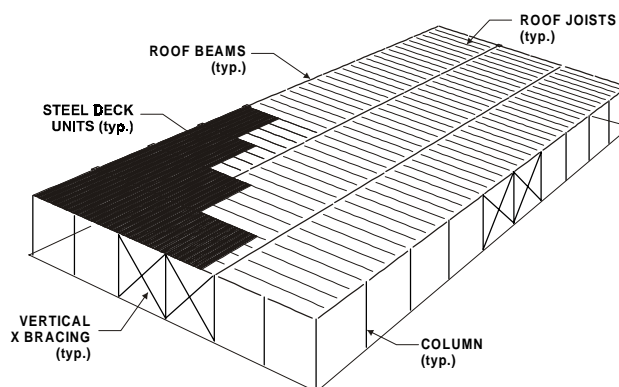

Figure 1: Typical low rise steel building

Several analytical investigations have shown that the in-plane flexibility of roof and floor diaphragms influences significantly the dynamic response of building structures to seismic ground motions [e.g. Dubina, 1997; Jain and Jennings, 1985; Medhekar, 1997; Naman and Goodno, 1986; Tena-Colunga,

[1]   Dept. of Civil, Geological and Mining Engineering, Ecole Polytechnique, Canada e-mail: tremblay@struc.polymtl.ca
[2]   Dept. of Civil, Geological and Mining Engineering, Ecole Polytechnique, Canada e-mail: rabih@hotmail.com
[3]   Dept. of Applied Mechanics and Engineering Science, University of California, USA, e-mail: afiliatr@soemail.ucsd.edu

1996; Tremblay and Stiemer, 1996; Tremblay, 1996]. The fundamental period of vibration of these structures is generally longer than equivalent buildings with rigid roof diaphragms and forces and deformations that develop in the diaphragms are also amplified due to dynamic effects. Similar amplifications have been observed by Celebi *et al.* [1986] in a single-storey building under the 1984 Morgan Hill earthquake.

Current design provisions in the National Building Code of Canada (NBCC) [NRCC, 1995] do not account for in-plane flexibility of roof diaphragms. For instance, the fundamental period of structures is evaluated based on the characteristics of the vertical bracing only. Minimum static lateral loads are specified in the code with no amplification factor to account for the in-plane dynamic response of the diaphragm. Provisions for horizontal torsion are also based on the assumptions that the diaphragms exhibit infinite in-plane stiffness. Similarly, design procedures for the design of steel roof deck diaphragms are essentially based on a static response of the diaphragm [CSSBI, 1991; Luttrell, 1991; ECCS, 1978].

An extensive shake table test program has been recently completed at École Polytechnique of Montreal on a 1:7.5 scale steel building model with a metal roof deck diaphragm. The objectives of this research were to obtain experimental data on the inelastic response of these structures under severe ground shaking, including the effects of the flexibility of the roof diaphragm, the strain rate effects on the yield strength of the vertical bracing, and the effects of in-plane eccentricities. The parameters investigated included two different sites: Victoria, B.C., and Quebec, Qc, which led to different ground motion characteristics and roof seismic weight values, two levels of flexibility for the diaphragm, and four eccentricity conditions: no eccentricity, mass eccentricity, stiffness eccentricity, and strength eccentricity. This paper describes the design of the test model and presents some of the main findings of this project.

TEST MODEL AND TEST PROCEDURE

Prototype building

Figure 2 shows the 30 m x 60 m x 6.6 m prototype building considered in the study. As shown, the roof framing is made of 30 m span trusses, spaced 7.5 m apart, which support steel joists at 1.875 m o/c. Perimeter beams are W shapes supported on HSS columns. The vertical bracing is made of tension-only diagonal members located along the four exterior walls. The structure was designed according to the NBCC and CSA-S16.1 [CSA, 1994] specifications. The specified seismic lateral load for the structure, V, is given by:

$$V = vSIFW\left(\frac{U}{R}\right)$$

where v is the zonal velocity ratio for the site (= 0.30 for Victoria and 0.15 for Quebec), S is the seismic response factor, I is the importance factor, F is the foundation factor, W is the seismic weight of the structure, U is a calibration factor (U = 0.6), and R is the force modification factor. The value of S depends upon the fundamental period of the structure and the seismic zones for the sites. For this type of building, the NBCC fundamental period, T, is equal to $0.09h_n/\sqrt{D_s}$, where h_n is the total height of the building (6.6 m) and D_s is the width of the lateral load resisting system (15 m). The period was then equal to 0.15 s, which led to S factors equal to 3.0 and 4.2 for Victoria and Quebec, respectively. For both sites, the importance factor and foundation factor were taken as 1.0. The seismic weight, W, only included the weight of the roof plus 25 % of the roof snow load: 1.25 kPa for Victoria and 1.785 kPa for Quebec. An R factor of 2.0 was used, assuming the vertical bracing met the provisions for steel concentrically braced frames with nominal ductility.

The total seismic load obtained from (1) was equal to 608 kN for both sites and, hence, the same lateral load resisting system could be used for both Victoria and Quebec. As described later, the computed fundamental period of the structure was much longer than the value of 0.15 s and the total seismic load could be reduced to 80% of 608 kN, i.e., 486 kN. At the design stage, the building was assumed to be perfectly symmetric and accidental eccentricity effects were omitted. For both sites, wind loading did not govern the design.

Each diagonal bracing member was sized to merely resist half the total seismic lateral load, which resulted in a brace cross-section area of 1030 mm^2, assuming F_y = 350 MPa. The diaphragm was to remain essentially under the design base earthquake and, hence, was designed to sustain a factored shear force corresponding to 110 % of the full yield load of the braces. The 10% increase accounts for impact loading likely to develop in tension-only bracing, as specified in the S16.1 provisions. The selected roof deck was made of intermediate rib, 38 mm deep x 914 mm wide sheets, with welded sidelap and frame connectors. Several combinations of metal thickness and fastener patterns could be used to develop the required shear resistance. For the more common 0.76 mm and 0.91 mm thick metals, the shear stiffness, G', of the various possible diaphragm designs, as obtained from the SDI Design Manual [Luttrell, 1991], varied between 3.11 kN/mm and 12.1 kN/mm.
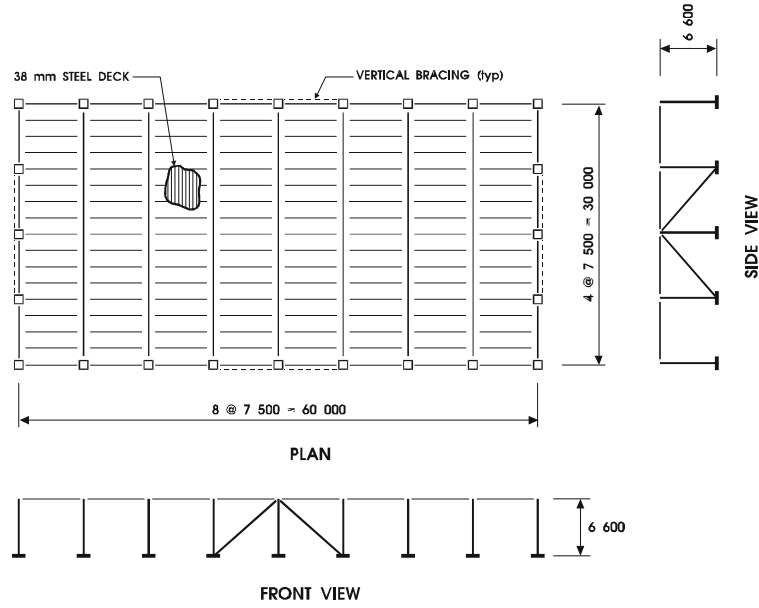
Figure 2: Building prototype

Of interest in this research was the behaviour of this structure when loaded in the direction perpendicular to the long (60 m) walls. The fundamental period of this type of structure can be estimated with the following expression adapted from Medhekar [1997]:

$$T = 2\pi\sqrt{\frac{\left(K_B + K_D\right)}{K_B K_D}\frac{W}{g}} \qquad \text{, with: } K_D = \frac{\pi^2}{\dfrac{L^3}{\pi^2 EI} + \dfrac{L}{G'b}} \qquad (2)$$

and where K_B is the total lateral stiffness of the vertical bracing in the direction considered, g is the acceleration due to gravity, and L, EI, and b are respectively the length (60 m), the bending stiffness, and the depth (30 m) of the roof diaphragm. For this structure, K_B was equal to 22 kN/mm and I was taken as 2.38×10^{12} mm^4, assuming W200x42 beams were used along the 60 m walls for both sites. The fundamental period computed with (2) varies between 0.78 s and 1.02 s for Victoria and between 0.93 s and 1.22 s for Quebec, respectively, for the possible range of G' . The interstorey drift at mid-span of the diaphragm includes the deformation of the vertical bracing, Δ_B, the bending deformation of the diaphragm, Δ_F, and the shear deformation of the diaphragm, Δ_S. Assuming V is uniformly distributed along the building length, these deformations under the 486 kN seismic design load are: $\Delta_B = 22$ mm, $\Delta_S = 2.9$ mm, and $\Delta_S = 10$ to 39 mm, depending upon the value of G' .

Model building

A first order model with artificial mass-simulation [Moncraz and Krawinkler, 1981] of the prototype building was designed and built for the test program. The set of dimensionless products that governed the choice of the target properties for the model were:

$$G\left(\frac{a}{g}, \frac{m'g}{E}, \frac{F_y}{E}, t\sqrt{\frac{E}{m'l}}, \frac{G'}{El}\right) = 0 \qquad (3)$$

where: a = acceleration, m' = mass per unit area of the roof, E = Young modulus, F_y = yield strength, t = time, and l = length. The scale factor for length, l_r, was set equal to 1 / 7.5 due to physical limitations, g_r was taken as 1.0, and steel was used for the fabrication of the structural components of the model, i.e., $E_r = 1.0$. Therefore, a, m' , and F_y had to be the same as in the prototype ($a_r = m'_r = F_{yr} = 1.0$), the scale factor for the time, t_r, was equal to $l_r^{0.5} = 0.365$ and G'_r was equal to l_r.

Figure 3 shows the building model. The dimensions were set to match exactly l_r: 4 m x 8 m x 0.88 m. The gravity load carrying system was simplified to reduce the number of components without affecting the behaviour of the lateral load system. All beam-to-column connections and column-to-foundation connections were true pinned connections and, hence, lateral loads were entirely resisted by the roof diaphragm and the vertical bracing.
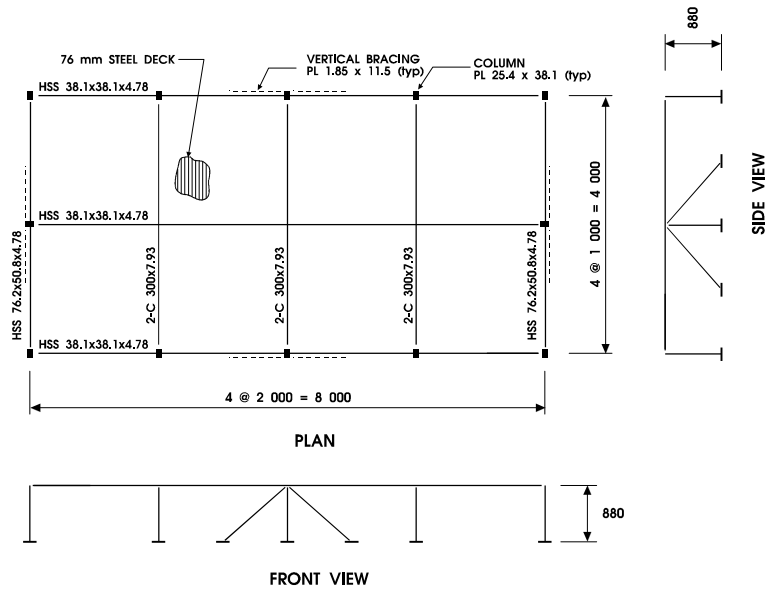
Figure 3: Building model

The target and selected values for the other parameters are given in Table 1. The selected roof mass values and properties for the diagonal bracing members deviated slightly from the target values due to physical constraints. The in-plane inertia of the roof was considerably higher than desired because the HSS members along the 8 m walls had to be designed to carry the weight of the roof. Such deviation was of limited consequence as the deformation Δ_F was relatively small for the prototype building (only 5-8% of the total drift). A Canam P2432 profile (narrow rib, 76 mm deep x 610 mm wide) made of 0.76 mm steel was selected for the roof deck. Sidelap connectors consisted of 10 button punches uniformly spaced over the depth of the diaphragm. The deck was connected to the HSS transverse beams with #14 self-drilling screws. Two different spacing values were considered: 305 mm o/c (flexible diaphragm) and 152 mm o/c (rigid diaphragm). The two values for G' in Table 1 correspond respectively to these two frame fastener patterns. These values were obtained with the method proposed in the SDI manual. The flexible diaphragm was selected to represent the prototype structure, whereas the tests with the rigid diaphragm configuration were to be used for comparison purposes.

Table 1 Properties of the building prototype and model.

Building	m'g (kPa)		Roof diaphragm		Diagonal bracing members		
	Victoria	Quebec	G' (kN/mm)	I (10^9 mm^4)	F_y (MPa)	A (mm^2)	$T_y=AF_y$ (kN)
Prototype	1.25	1.785	3.11 – 12.1	2380	350	1030	361
Model (target)	1.25	1.785	0.41 – 1.61	0.752	350	18.3	6.41
Model (selected)	1.381	1.859	0.69 & 3.34	4.34	314	21.3	6.69
Selected/target	1.10	1.04	-	5.77	0.90	1.16	1.04

Small (300 mm x 300 mm x 55 mm) concrete blocks were attached to the roof deck to simulate the mass at the roof level. The building model was supported on a stiff 4 m x 8 m dedicated steel frame that had been assembled on the 3.4 m x 3.4 m earthquake simulator. Earthquake ground motion was applied parallel to the short walls.

Modelling eccentricities

Mass eccentricity was simulated by moving the concrete blocks along the long direction of the building. Typical mass eccentricities varied between 0.07 L and 0.10 L. Stiffness and strength eccentricities were obtained by modifying the diagonal bracing members located in the short end walls. For the stiffness eccentricity, stiffer braces were used along one short wall whereas more flexible braces were placed in the opposite wall. The yield strength of both sets of braces was kept equal to 6.7 kN. Strength eccentricity was achieved by respectively

reducing and increasing the strength of the braces in the two opposite short walls while maintaining their stiffness equal to that of the original bracing members. Stiffness and strength eccentricities varied between 0.28 and 0.30 L.

Test procedure and instrumentation

Static tests and system identification tests were first performed to determine the structural and dynamic characteristics of the test model in its various configurations. In the static tests, the roof was attached to a fixed support at mid-span of the diaphragm and a quasi-static cyclic displacement corresponding to the ATC-24 procedure [ATC, 1992] was applied with the earthquake simulator. For the model with strength and stiffness eccentricities, the tests were limited to the elastic loading cycles in order not to damage the special bracing members. A low amplitude white noise signal was applied to determine the natural frequencies of the model and the damping characteristics were determined with the log-decrement technique. Thereafter, the model was subjected to a site specific ground motion time history. For Victoria, the N04O Olympia Highway Test Lab record of the 1949 Western Washington earthquake (M_L 7.1) was used. For Quebec City, a simulated ground motion produced by a M_w 7.0 event at 150 km was considered. Roof displacements and accelerations were measured at 5 locations along the diaphragm length. Load cells were installed in all bracing members to monitor the brace forces. X-mounted LVDTs were also used to measure shear deformations in the diaphragm at 4 locations along half the length of the roof.

TEST RESULTS

Stiffness and Dynamic Properties

The actual stiffness and strength of the bracing members corresponded well with the predicted values. However, the measured stiffness values of the roof diaphragm were significantly different from the theoretical values given in Table 1: 1.54 kN/mm and 1.94 kN/mm, for the flexible and rigid roof configurations, respectively. This suggests that the SDI method does not apply well to the roof diaphragm assemblies used in the study. Using the actual stiffness properties of the model, the fundamental period predicted by (2) agreed very well with the measured period. For instance, K_B of the building model for Victoria with the flexible diaphragm was equal to 3.28 kN/mm and both the measured and computed periods were found equal to 0.28 s. The measured first mode damping ratio of the model varied between 3.1% and 4.3%.

Interstorey drift under earthquake loading

Figure 4a presents the time history of the relative roof displacement measured at mid-span and at both ends (average) of the diaphragm for the Victoria site and the flexible diaphragm. In this test (#4), the ground motion was scaled to a peak velocity of 0.28 m/s. The figure shows that larger interstorey drift took place at mid-span of the diaphragm. In this test, the measured peak in-plane deformation of the roof was equal to 1.9 times the deformation computed assuming a static uniformly distributed load producing yielding of the bracing members is applied to the roof. Similar ratios varying between 1.63 and 1.93 were obtained in other tests performed in this study. Such dynamic amplification corresponds well with that observed in past analytical studies [e.g. Tremblay and Stiemer, 1996].

Strain rate effects under earthquake loading

Significant strain rate effects on the yield resistance of the bracing members were observed in the test program. Such effects can be visualised in the recorded brace hysteresis loops such as the one shown in Fig. 4b. In this example, the yield load reached 1.13 times the value measured in the static test. Comparable results were obtained in other braces and other tests. Of course, strain rates monitored in a scaled model are higher than in actual structures. For the case shown in Fig. 4b, the average strain rate near yielding was 0.05 s^{-1}. Applying the time scale factor (tr = 0.365) to this value gives a strain rate of 0.018 s^{-1} at the prototype scale. Using the expression by Wakabayashi et al. [1984], the ratio of the dynamic to static yield strength for these two strain rates are respectively 1.14 and 1.12. This indicates that actual bracing systems can also experience similar level of strain rate effects during strong ground shaking, which would result in higher lateral loads imposed on the roof diaphragm. The same conclusion was proposed by Tremblay and Filiatrault [1996].
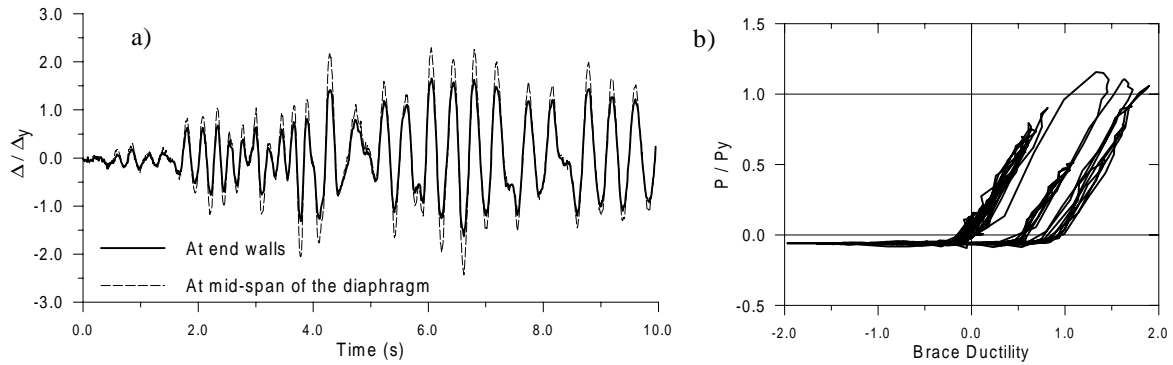
Figure 4: Response under test #4:
a) Time history of the relative roof displacement; b) Brace hysteresis

Shear forces in the roof diaphragm under earthquake loading

Shear forces acting in the diaphragm could be obtained from the shear deformations measured in the roof during the tests. The peak shear forces obtained in tests #4 and #5 are shown in Fig. 5 (test #5 is identical to test #4, except that the ground motion was scaled to 0.42 m/s). The distribution of shear assuming static loading conditions is also given in the figure. In addition, the results of nonlinear dynamic analyses duplicating the conditions of tests #4 and #5 are presented in the graph. As shown, both the measured and computed values exceed the static values. The shear forces also tend to increase when the amplitude of ground motion is increased. Note that the high experimental values near the end of the diaphragm may not be representative as they were computed assuming a linear relationship between shear deformations and shear forces in the diaphragm. In the quasi-cyclic tests, this assumption could only be verified up to V_y. Nevertheless, the experimental data confirm that shear forces larger than those predicted assuming static loading are likely to develop under earthquake loading. Figure 5 also shows that these shear forces could be estimated through nonlinear dynamic analysis.
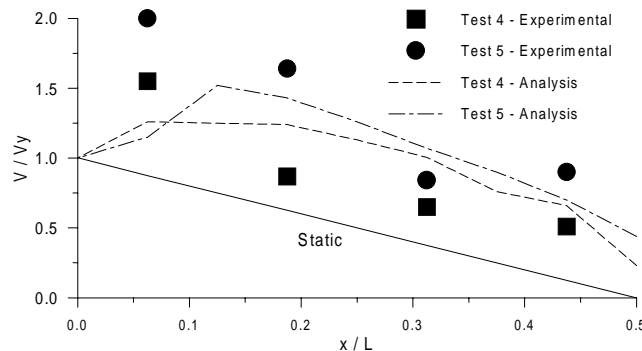

Figure 5: Shear forces in the roof diaphragm (Tests #4 & #5)

Eccentricity under earthquake loading

Current NBCC code provisions require that the eccentricity between the centre of mass and centre of rigidity be taken into account when assessing the forces acting in the various elements of the lateral load resisting system of building structures. This calculation is generally performed assuming the structure is elastic and the redistribution of the loads after yielding has developed in the elements is therefore ignored. There is no code provisions either to account for in-plane rotation that would result from an uneven (unbalanced) strength distribution between the lateral load resisting elements in a building. Nowadays, the inelastic torsional response of building structures can be examined using a static three-dimensional push-over analysis. In this type of analysis, however, the point of application of the lateral load is assumed to be located at the centre of mass, which may not be representative of the conditions under dynamic loading. In the test program, mass, stiffness, and strength eccentricity were intentionally created along the length of the building (L = 8.0 m), in the direction

perpendicular to the seismic excitation, and the peak tension forces that developed in the bracing members located in the long walls were measured and compared to the values predicted by a static analysis.

Test #6 was the same as test #4 except that the centre of rigidity (CR) was moved 0.24 L away from the centre of the building by using bracing members with a different stiffness in each of the two short walls. At the stiff end, the braces were 1.31 times stiffer than the braces located in the long walls. At the opposite end, the stiffness of the braces was equal to 46% of the stiffness of the longitudinal braces. The centre of mass (CM) was located at the centre of the building and all bracing members had the same tensile yield load, T_y. A push-over analysis shows that the tension force in the longitudinal braces reaches 0.23 T_y when yielding initiates in the stiffer end braces. The CR then shifts at the flexible end wall location and the force in the long wall braces decreases until yielding occurs in the flexible end braces.

In the test, the braces in both short walls experienced several yield excursions with a peak ductility of 3.8 for the stiffer braces and 2.5 for the flexible ones. During the first few inelastic cycles, which took place between 4 and 4.6 s of ground motion, peaks in tension load ranging from 0.15 to 0.29 T_y were recorded in the longitudinal braces. This agrees well with the prediction of the static analysis. In the subsequent yielding cycles, between approximately 4.6 s and 8 s of excitation, tension forces varying between 0.23 and 0.39 T_y developed in the braces located in the long walls. These higher forces are attributed to large torsional moments induced by the dynamic nature of the building response, as governed by the highly nonlinear behaviour of the yielded bracing members. After yielding of the braces, the position of the CR continually moves when the building oscillates, depending upon the stiffness condition of the end braces (slack, elastic, yielding). The position of the inertia loads is also found to move due to the variation of the roof horizontal acceleration along the length of the diaphragm. For example, Fig. 6 shows the position of the lateral load determined from roof acceleration measurements during the strong ground motion part of the record (4 - 9 s). As shown, the assumption that the load is applied at the CM does not hold and the movement of CR relative to CM creates eccentricity conditions that cannot be predicted with a static analysis, even for a simple building as the one examined in this study.
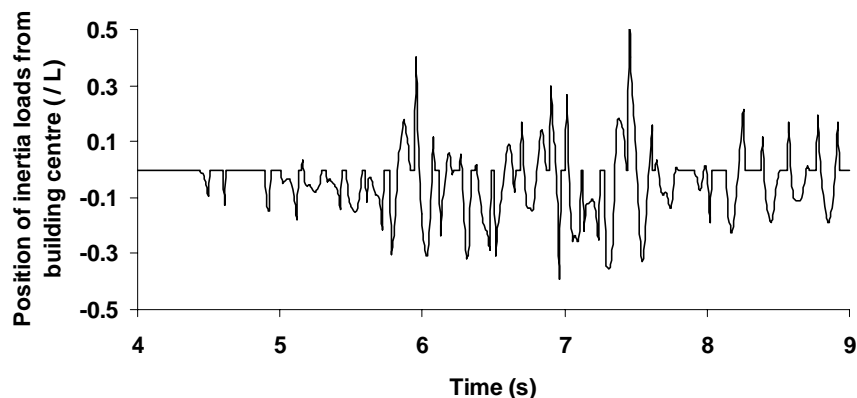

Figure 6: Variation of the position of the inertia loads with time (Test #6)

In test #7, strength eccentricity equal to 0.30 L was introduced in the model with a flexible diaphragm for Victoria. The bracing members had a yield strength of 13.4 kN in one short wall and 3.35 kN in the opposite wall. In the longitudinal walls, T_y of the braces was equal to 6.7 kN. Both the CM and CR were located at the centre of the building (all braces had the same stiffness). The ground motion was scaled to a peak velocity of 0.20 m/s. A push-over analysis indicates that no force develops in the longitudinal braces until yielding occurs in the weak end braces. The longitudinal braces then yield when the tension load in the strong end braces reaches 7.6 kN. During the test, a peak ductility demand of 5.7 was observed in the weak braces whereas the stronger braces remained elastic, with a peak load of 7.6 kN. Up to yielding of the weak braces, no force was recorded in the longitudinal braces, as expected. After yielding had taken place, tension forces up to 0.35 T_y were recorded in the longitudinal braces, which is lower than predicted by the static analysis when the force in the strong end braces reach 7.6 kN. Again, the measurements showed a significant movement of the point of application of the inertia loads, which most likely influenced the distribution of the forces in the vertical bracing elements.
Also of interest is the comparison of tests #4 and #6. In the former, the total yield lateral resistance provided by the end braces was equal to 10.1 kN (12.6 kN in test #6) and the ground motion was scaled to 0.28 m/s (0.20 m/s in test #6). Hence, the strength demand to supply ratio in test #4 was higher than in test #6. The measured peak ductility levels in the braces were 1.97 and 5.7 for tests #4 and #6, respectively, which indicates that strength

eccentricity can have a significant impact on the inelastic response of building structures and should be accounted for in design.

CONCLUSION

Shake table tests were performed to examine the seismic performance of low-rise steel buildings with flexible roof diaphragms. It was shown that the fundamental period of these structure can be estimated using a simplified formula that has been proposed in the literature. The tests also confirmed the findings of past analytical studies regarding the dynamic amplification of the deformations and shear forces in the roof diaphragm. The measured shear force levels could be reproduced by nonlinear dynamic analyses. The high strain rates experienced by the bracing members increased their yield resistance and, hence, contributed in the higher forces imposed to the roof diaphragm. Strength eccentricity was found to have a strong impact on the ductility demand on the vertical bracing elements. Numerical models should be calibrated against this test data set in order to extend the scope of this study and improve further the understanding of the seismic behaviour of these structures.

ACKNOWLEDGEMENTS

REFERENCES

ATC. 1992. ATC-24, Guidelines for Cyclic Seismic Testing of Components of Steel Structures, Applied Technology Council, Redwood City, Ca.

Celebi, M., Bongiovanni, G., Safak, E., and Brady, G. 1989. Seismic Response of a Large-Span Roof Diaphragm. Earthquake Spectra, 5, 337-350.

CSA. 1994. CSA-S16.1-94. Limit States Design of Steel Structures. Canadian Standard Association, Rexdale, Ont.

CSSBI. 1991. Design of Steel Deck Diaphragms. Canadian Sheet Steel Building Institute, Willowdale, Ont.

Dubina, D., Zaharia, R. and Georgescu, M. 1997. Stress Skin Design of Single-Storey Steel Buildings in Seismic Areas. Proc. STESSA '97 Conf. on the Behaviour of Steel Struct. in Seismic Areas. Kyoto, Japan, 426-433.

ECCS. 1978. Recommendations for Steel Construction – ECCS TC7 – The Stressed Skin Design of Steel Structures. European Convention for Constructional Steelwork, Publ. 19, Rotterdam, Holland.

Jain, S.K. and Jennings, P.C. 1985. Analytical models for low-rise buildings with flexible roof diaphragms. Earthquake Engineering and Structural Dynamics, 13, 225-241.

Luttrell, L.D. 1991. Diaphragm Design Manual, 2nd ed., Steel Deck Institute, Inc., Canton, Ohio.

Medhekar, M.S. 1997. Seismic Evaluation of Steel Buildings with Concentrically Braced Frames. Ph.D. Thesis, Dept. of Civil and Environmental Engrg., Univ. of Alberta, Edmonton, Alberta.

Moncarz, P.D. and Krawinkler, H. 1981. Theory and Application of Experimental Model Analysis in Earthquake Engineering. Report no. 50, John A. Blume Earthquake Engineering Center, Stanford University, San Francisco, Ca.

Naman, S.K. and Goodno, B.J. 1986. Seismic Evaluation of Low Rise Steel Building. Engrg. Struct., 8, 9-16.

NRCC. 1995. National Building Code of Canada (NBCC), 11th ed., Associate Committee on the National Building Code, National Research Council of Canada (NRCC), Ottawa, Ont.

Tena-Colunga, Abrams, D.P. 1996. Seismic Behavior of Structures with Flexible Diaphragms. J. of Struct. Eng., ASCE, 122, 439-445.

Tremblay, R. and Filiatrault, A. 1996. Seismic Impact Loading in Inelastic Tension-only Concentrically Braced Steel Frames: Myth or Reality? Earth. Engrg. and Struct. Dyn., 25, 1373-1389.

Tremblay, R. and Stiemer, S.F. 1996. Seismic Behavior of Single-Storey Steel Structures with Flexible Diaphragm. Can. J. of Civ. Engrg., 23, 49-62.